DALTON

Synthesis, structure, spectra and redox chemistry of iron(III) complexes of tridentate pyridyl and benzimidazolyl ligands †

Rathinam Viswanathan, Mallayan Palaniandavar,* Thailampillai Balasubramanian and P. Thomas Muthiah

Department of Chemistry, Bharathidasan University, Tiruchirappalli 620 024, Tamil Nadu, India

A series of high-spin octahedral 1:2 iron(III) complexes of Schiff bases derived from salicylaldehyde and aromatic amines and the 1:1 and 1:2 complexes of bis(pyridin-2-yl)-aza and bis(benzimidazol-2-yl)-aza and -thioether ligands have been isolated. The crystal structure of trichloro[bis(pyridin-2-ylmethyl)amine]iron(III) has been determined. It contains two crystallographically independent molecules in the asymmetric unit cell. In each molecule iron(III) possesses a rhombically distorted octahedral co-ordination, constituted by all the three nitrogens of the facial ligand and three chloride ions. The effects of stereochemical and/or donor atom variations on the UV/VIS and EPR spectra and Fe^{III}–Fe^{II} redox potentials and hence on the Lewis acidity of the iron(III) centre are discussed. The phenolate-to-iron(III) charge-transfer band energy of $[FeL^1{}_2]Cl$ [HL^1 = *N*-(pyridin-2-ylmethyl)salicylideneamine] is higher and its Fe^{III}–Fe^{II} redox potential more negative than those of the corresponding 1:1 complex.

Several iron(III) complexes[1-4] have been isolated and studied as models to elucidate the structure–function relationship of iron(III) tyrosinate proteins.[5-7] Two[1,2] of these contain but one co-ordinated phenolate donor and another compound[3] both the established imidazole-derived nitrogen and phenolate donors of the tyrosinate enzymes.[6,7] Further, the iron(III)–salen model complex[4] [H_2salen = *N*,*N*′-bis(salicylidene)ethane-1,2-diamine] which contains two co-ordinated phenolate groups is planar, whereas the active sites in the enzymes are non-planar (non-haem).[6] So we became interested in synthesising and studying non-planar iron(III) chelates containing two co-ordinated phenolate oxygen donors. We have found[8] that the presence of two phenolate donors in the iron(III) complexes of tetradentate tripodal ligands enhances the dioxygenase activity of the enzymes. To incorporate two co-ordinated phenolate functions in the present study we have employed the simple strategy of using linear tridentate phenolate ligands[9] to prepare bis complexes.

The present Schiff bases, though simple, vary systematically in order to understand the effect of donor-atom types on the phenolate-to-iron(III) charge-transfer spectra and hence to obtain meaningful information about factors affecting the Lewis acidity of the iron(III) centre located in grossly similar stereochemistries. Since the dioxygenase activity of tyrosinate enzymes is considered to be intimately related to their ease of reduction, and in turn to their iron co-ordination environment, the study of the redox properties of the iron(III) complexes and their correlation with donor-atom type became our main endeavour. There have been few systematic studies on the sensitivity of Fe^{III}–Fe^{II} redox potentials to variations of ligand donor-atom types in high-spin iron(III) complexes[10] and Lever[11] has pointed out that the redox potential data base for six-co-ordinate high-spin iron(III) complexes is rather limited. So the redox behaviour of 1:1 and 1:2 iron(III) complexes of the related non-phenolate bis(pyridin-2-yl) and bis(benzimidazol-2-yl) ligands containing aza (N_3) and thioether (N_2S) donors has also been investigated. Finally we report the novel structure of one of these complexes in which bis(pyridin-2-ylmethyl)amine is folded facially to co-ordinate to iron(III).

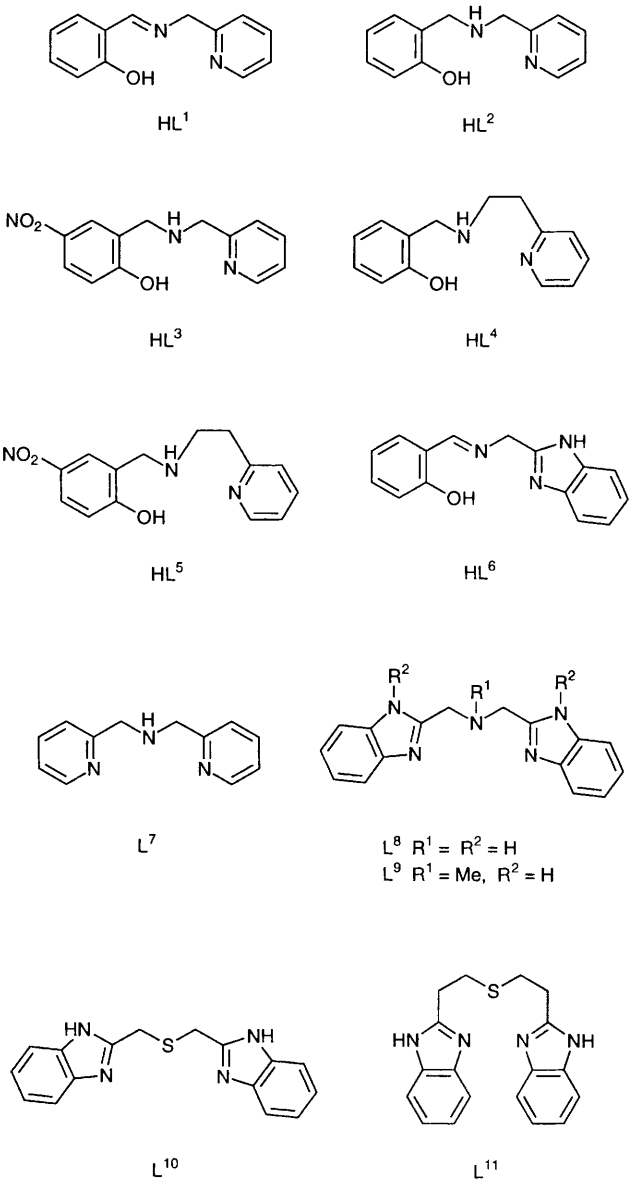

† *Non-SI units employed:* $\mu_B \approx 9.27 \times 10^{-24}$ J T^{-1}, G = 10^{-4} T.

Experimental

Materials

Iron(III) chloride (anhydrous) and triethylamine (S. D. Fine Chemicals, India) were analytical grade reagents used as supplied. *o*-Phenylenediamine, β-alanine, salicylaldehyde (BDH) and sodium tetrahydroborate (Fluka), and 2-(chloromethyl)benzimidazole, 2-(aminomethyl)pyridine, 2-(aminoethyl)pyridine and 2-(chloromethyl)pyridine hydrochloride (Aldrich) were used as received. The supporting electrolyte tetra-*n*-hexylammonium perchlorate (GFS) was recrystallised twice from aqueous ethanol and dried over P_4O_{10}.

2-(Aminomethyl)benzimidazole dihydrochloride,[12] 2-(aminoethyl)benzimidazole dihydrochloride[12] and 2-hydroxy-5-nitrobenzyl chloride,[13] bis(benzimidazol-2-ylmethyl)amine[14] (L^8), bis(benzimidazol-2-ylmethyl)methylamine[14] (L^9), bis(benzimidazol-2-ylmethyl) sulfide[15] (L^{10}) and bis(benzimidazol-2-ylethyl) sulfide[16] (L^{11}) were prepared using published procedures.

Syntheses of iron(III) complexes

$[FeL^1_2]Cl$ [HL^1 = *N*-(pyridin-2-ylmethyl)salicylideneamine]. To a solution of 2-(aminomethyl)pyridine (0.44 g, 4 mmol) in tetrahydrofuran (thf) (25 cm^3) was added salicylaldehyde (0.49 g, 4 mmol) and refluxed for 30 min. This was then cooled and filtered. To the filtrate NEt_3 (0.40 g, 4 mmol) and then $FeCl_3$ (0.32 g, 2 mmol) in methanol (5 cm^3) were added and the solution cooled. The dark brown precipitate obtained was filtered off, washed with small amounts of cold methanol and dried over P_4O_{10} under vacuum. Yield 0.40 g (78%).

$[FeL^2_2]Cl$ [HL^2 = (2-hydroxybenzyl)(pyridin-2-ylmethyl)amine]. Salicylaldehyde (0.25 g, 2 mmol) was added to a solution of 2-(aminomethyl)pyridine (0.22 g, 2 mmol) in thf (25 cm^3) and then refluxed for 30 min. This was cooled and $NaBH_4$ (0.08 g, 2 mmol) was added with stirring. The solution was filtered and then rotaevaporated. Methanol (15 cm^3) was added to dissolve the residue, followed by NEt_3 (0.20 g, 2 mmol) and $FeCl_3$ (0.16 g, 1 mmol) in methanol (5 cm^3) and the solution was cooled. The dark brown precipitate obtained was filtered off, washed with small amounts of cold methanol and dried over P_4O_{10} under vacuum. Yield 0.44 g (85%).

$[FeL^3_2]Cl$ [HL^3 = *N*-(2-hydroxy-5-nitrobenzyl)(pyridin-2-ylmethyl)amine]. To a solution of 2-hydroxy-5-nitrobenzyl chloride (0.38 g, 2 mmol) in thf (50 cm^3) were added 2-(aminomethyl)pyridine (0.22 g, 2 mmol) and NEt_3 (0.20 g, 2 mmol) and then refluxed for 2 h. This was then cooled and filtered. The filtrate was rotaevaporated and methanol (5 cm^3) followed by NEt_3 (0.20 g, 2 mmol) were added. To this solution $FeCl_3$ (0.16 g, 1 mmol) in methanol (5 cm^3) was added. The brown precipitate obtained was filtered off, washed with small amounts of cold methanol and dried over P_4O_{10} under vacuum. Yield 0.53 g (87%).

$[FeL^4_2]Cl$ [HL^4 = *N*-(2-hydroxybenzyl)(pyridin-2-ylethyl)amine] and $[FeL^5_2]Cl$ [HL^5 = (2-hydroxy-5-nitrobenzyl)(pyridin-2-ylethyl)amine]. These were prepared adopting the procedures employed for $[FeL^2_2]Cl$ and $[FeL^3_2]Cl$ respectively and using 2-(aminoethyl)- instead of 2-(aminomethyl)-pyridine. Yields 0.48 (87) and 0.58 g (92%) respectively.

$[FeL^6_2]Cl$ [HL^6 = (benzimidazol-2-ylmethyl)salicylideneamine]. Salicylaldehyde (0.24 g, 2 mmol) in methanol (25 cm^3) and then NEt_3 (0.40 g, 4 mmol) were added to a solution of 2-(aminomethyl)benzimidazole dihydrochloride (0.44 g, 2 mmol) in methanol (25 cm^3) and refluxed for 30 min. The solution was cooled, filtered, and then NEt_3 (0.20 g, 2 mmol) was added followed by $FeCl_3$ (0.16 g, 1 mmol). The brown precipitate obtained on cooling was filtered off, washed with small amounts of cold methanol and dried under vacuum. Yield 0.36 g (61%).

$[FeL^7Cl_3]$ [L^7 = bis(pyridin-2-ylmethyl)amine]. To a solution of bis(pyridin-2-ylmethyl)amine (0.20 g, 1 mmol) in methanol (10 cm^3) was added $FeCl_3$ (0.16 g, 1 mmol) in methanol (5 cm^3), stirred and cooled. The yellow precipitate obtained was filtered off, washed with small amounts of cold methanol and dried over P_4O_{10} under vacuum. Yield 0.28 g (86%). A methanolic solution of the complex, on slow evaporation, yielded yellow crystals suitable for X-ray diffraction studies.

$[FeL^7_2]Cl_3$. To a solution of bis(pyridin-2-ylmethyl)amine (0.40 g, 2 mmol) in methanol (10 cm^3) was added $FeCl_3$ (0.16 g, 1 mmol) in methanol (5 cm^3), stirred and cooled. The yellow precipitate obtained was filtered off, washed with small amounts of cold methanol and dried over P_4O_{10} under vacuum. Yield 0.51 g (91%).

$FeL^8_2Cl_3$ [L^8 = bis(benzimidazol-2-ylmethyl)amine]. This was prepared according to the procedure employed for $FeL^7_2Cl_3$. Yield 0.58 g (81%).

$[FeL^8Cl_3]$ and $[FeL^9Cl_3]$ [L^9 = bis(benzimidazol-2-ylmethyl)-methylamine]. These complexes were prepared as reported already.[17]

$FeL^9_2Cl_3$. This complex was prepared using the method adopted for $[FeL^7_2]Cl_3$. Yield 0.54 g (72%).

$[FeL^{10}Cl_3]$ [L^{10} = bis(benzimidazol-2-ylmethyl) sulfide]. To a solution of bis(benzimidazol-2-ylmethyl) sulfide (0.29 g, 1 mmol) in methanol (25 cm^3) was added $FeCl_3$ (0.16 g, 1 mmol) in methanol (5 cm^3) with stirring and then cooled. The yellow precipitate was filtered off, washed with small amounts of cold methanol and dried over P_4O_{10} under vacuum. Yield 0.38 g (83%).

$[FeL^{10}_2]Cl_3$. To a solution of bis(benzimidazol-2-ylmethyl) sulfide (0.59 g, 2 mmol) in methanol (25 cm^3) was added $FeCl_3$ (0.16 g, 1 mmol) in methanol (5 cm^3) with stirring and then cooled. The yellow precipitate was filtered off, washed with small amounts of cold methanol, and dried over P_4O_{10} under vacuum. Yield 0.52 g (76%).

$[FeL^{11}Cl_3]$ and $[FeL^{11}_2]Cl_2$ [L^{11} = bis(benzimidazol-2-ylethyl) sulfide]. These complexes were isolated by the methods employed for $[FeL^{10}Cl_3]$ and $[FeL^{10}_2Cl_3]$ respectively and using L^{11} instead of L^{10}. Yields 0.31 (66) and 0.61 g (83%) respectively.

Physical measurements

Elemental analyses were performed at Hindustan Photo Film Manufacturing Co. Ltd., Ootacamund and Regional Sophisticated Instrumentation Centre, Lucknow, India. Electronic spectra were recorded on a Hitachi U-3410 double-beam UV–VIS–NIR spectrophotometer, EPR spectra on a Varian E 112 X-band spectrometer, the field being calibrated with diphenylpicrylhydrazyl (dpph). All voltammetric experiments were performed in a single-compartment cell with a three electrode system on a EG & G PAR 273 potentiostat/galvanostat equipped with an IBM PS/2 computer and a HIPLOT DMP-40 series digital plotter. The working electrode was a glassy carbon disc (area 0.283 cm^2) and the reference a saturated calomel

Table 1 Elemental analyses of iron(III) complexes with calculated values in parentheses

Compound	Analysis (%)			
	C	H	N	Fe
$[FeL^1{}_2]Cl$	60.45	4.20	10.80	10.65
	(60.80)	(4.30)	(10.90)	(10.85)
$[FeL^2{}_2]Cl$	60.15	4.95	10.65	10.90
	(60.30)	(5.05)	(10.80)	(10.80)
$[FeL^3{}_2]Cl$	51.25	3.95	13.75	8.90
	(51.40)	(4.00)	(13.85)	(9.20)
$[FeL^4{}_2]Cl$	61.50	5.50	10.20	10.15
	(61.60)	(5.55)	(10.25)	(10.25)
$[FeL^5{}_2]Cl$	52.75	4.40	13.10	9.40
	(52.90)	(4.45)	(13.20)	(9.45)
$[FeL^6{}_2]Cl$	53.20	3.80	13.25	8.70
	(53.25)	(3.85)	(13.30)	(8.80)
$[FeL^7Cl_3]$	39.85	3.60	11.60	15.75
	(39.85)	(3.60)	(11.65)	(15.45)
$[FeL^7{}_2Cl_3]$	51.40	4.65	14.85	9.75
	(51.40)	(4.65)	(15.00)	(9.95)
$FeL^8{}_2Cl_3$	53.55	4.15	19.50	7.75
	(53.60)	(4.20)	(19.55)	(7.80)
$FeL^9{}_2Cl_3$	54.80	4.55	18.75	7.45
	(54.80)	(4.60)	(18.80)	(7.50)
$[FeL^{10}Cl_3]$	42.05	3.10	12.30	12.15
	(42.10)	(3.10)	(12.25)	(12.25)
$[FeL^{10}{}_2Cl_3]$	51.15	3.75	14.90	7.40
	(51.20)	(3.75)	(14.90)	(7.45)
$[FeL^{11}Cl_3]$	44.60	3.70	11.40	11.50
	(44.60)	(3.75)	(11.55)	(11.50)
$[FeL^{11}{}_2Cl_3]$	53.55	4.60	13.85	6.85
	(53.60)	(4.50)	(13.90)	(6.90)

electrode. A platinum plate was used as the counter electrode. The supporting electrolyte used was 0.1 mol dm^{-3} NBu_4ClO_4. Solutions were deoxygenated by purging with N_2 gas for 15 min prior to and during measurements. The temperature of the methanol solution was maintained at 25 ± 0.2 °C by a Haake D8 G circulating bath. The potential of the ferrocene–ferrocenium couple (0.100 V *vs.* $Ag-Ag^+$) was measured in methanol under the same identical conditions to enable correction for junction potentials.

Crystallography

Preliminary cell dimensions of $[FeL^7Cl_3]$ and the crystal system were determined and refined on an Enraf-Nonius CAD4 X-ray diffractometer. The intensities were collected at 295 K with graphite-monochromated Mo-Kα radiation (λ 0.710 69 Å). The crystal data and details of data collection are summarized in Table 1. The intensity of representative reflections were measured after every 100 reflections. No decay correction was required. The data were corrected for Lorentz and polarisation effects. An empirical absorption correction based on ψ scans was applied. Systematic absences of reflections of the type $0k0$ ($k = 2n + 1$) and $h0l$ ($l = 2n + 1$) suggested the space group $P2_1/c$ unambiguously. The E statistics also suggested this space group and it was confirmed by the successful refinement. The structure was solved using the SHELXS 86 program[18] and refined with SHELXL 93.[19] The refinement was performed on F^2. The coordinates of hydrogen atoms were refined with their isotropic temperature factors assigned with a value of 0.05 $Å^2$. The weighting scheme used was $w^{-1} = [\sigma^2(F_o^2) + (0.1290P)^2 + 21.96P]$ where $P = \max.[(F_o^2, 0) + 2F_c^2]/3$. Structural parameters like bond lengths, angles, *etc.* were calculated using the program PARST.[20] All the calculations were carried out using MICROVAX-II. Selected bond lengths and angles are in Table 2.

Atomic coordinates, thermal parameters and bond lengths and angles have been deposited at the Cambridge Crystallographic Data Centre (CCDC). See Instructions for Authors, *J. Chem. Soc., Dalton Trans.*, 1996, Issue 1. Any request to the CCDC for this material should quote the full literature citation and the reference number 186/63.

Table 2 Crystal data for $[FeL^7Cl_3]$

Empirical formula	$C_{12}H_{13}Cl_3FeN_3$
M	361
Crystal system	Monoclinic
Space group	$P2_1/c$
a/Å	23.810(8)
b/Å	8.480(2)
c/Å	15.620(9)
β/°	107.46(4)
U/$Å^3$	3009
Z	8
Crystal dimensions/mm	0.18 × 0.27 × 0.21
D_c/g cm^{-3}	1.569
$F(000)$	1416.0
Scan type	ω–2θ
Scan rate	5.0° min^{-1} (in ω), up to 3 scans
No. reflections measured	Total 4832
R, R'	Unique 4545 (R_{int} = 0.0168) 0.089, 0.250

Table 3 Selected bond distances (Å) and angles (°) for $[FeL^7Cl_3]$

Fe–Cl(1)	2.277(4)	Fe(A)–Cl(1A)	2.319(5)
Fe–Cl(2)	2.317(4)	Fe(A)–Cl(2A)	2.274(4)
Fe–Cl(3)	2.283(5)	Fe(A)–Cl(3A)	2.293(4)
Fe–N(1)	2.168(14)	Fe(A)–N(1A)	2.197(14)
Fe–N(8)	2.216(13)	Fe(A)–N(8A)	2.208(12)
Fe–N(15)	2.172(13)	Fe(A)–N(15A)	2.194(13)
N(8)–Fe–N(15)	76.2(5)	N(8A)–Fe(A)–N(15A)	77.1(5)
N(1)–Fe–N(15)	78.6(5)	N(1A)–Fe(A)–N(15A)	80.1(5)
N(1)–Fe–N(8)	75.9(5)	N(1A)–Fe(A)–N(8A)	76.1(5)
Cl(3)–Fe–N(15)	92.1(4)	Cl(2A)–Fe(A)–N(15A)	94.7(3)
Cl(3)–Fe–N(8)	89.8(4)	Cl(2A)–Fe(A)–N(8A)	167.4(4)
Cl(3)–Fe–N(1)	164.3(4)	Cl(2A)–Fe(A)–N(1A)	93.2(4)
Cl(2)–Fe–N(15)	161.7(4)	Cl(1A)–Fe(A)–N(15A)	87.2(3)
Cl(2)–Fe–N(8)	89.5(4)	Cl(1A)–Fe(A)–N(8A)	90.9(4)
Cl(2)–Fe–N(1)	87.0(4)	Cl(1A)–Fe(A)–N(1A)	163.5(4)
Cl(2)–Fe–Cl(3)	99.3(2)	Cl(1A)–Fe(A)–Cl(2A)	98.4(2)
Cl(1)–Fe–N(15)	94.4(4)	Fe(A)–N(1A)–C(6A)	117.0(11)
Cl(1)–Fe–N(8)	167.4(3)	Fe(A)–N(1A)–C(2A)	124.1(11)
Cl(1)–Fe–N(1)	94.3(4)	Fe(A)–N(8A)–C(7A)	109.2(11)
Cl(1)–Fe–Cl(3)	99.0(2)	Fe(A)–N(8A)–C(9A)	112.0(10)
Cl(1)–Fe–Cl(2)	97.9(2)	Fe(A)–N(15A)–C(14A)	125.0(10)
Fe–N(1)–C(6)	116.4(10)	Fe(A)–N(15A)–C(10A)	116.3(10)
Fe–N(1)–C(2)	125.0(11)		
Fe–N(8)–C(9)	108.0(10)		
Fe–N(15)–C(10)	117.6(11)		
Fe–N(8)–C(7)	111.6(10)		
Fe–N(15)–C(14)	123.4(11)		

Results and Discussion

On the basis of the elemental analysis (Table 1) the formula of the present iron(III) phenolate complexes may be represented as $[FeL_2]Cl$ and the mono- and bis-chelates of the triaza (N_3) and N_2S ligands as $[FeL]Cl_3$ and $[FeL_2]Cl_3$ respectively. The phenolates chosen are derived from salicylaldehyde so as to provide a systematic variation in the nature of donor atoms and to vary the Lewis acidity of the iron(III) centre in high-spin six-co-ordinate complexes.

Crystal structure of $[FeL^7Cl_3]$

The crystals were grown from methanol solution as yellow prisms in the space group $P2_1/c$. The structure of the molecule is shown in Fig. 1, together with the atom numbering scheme. There are two crystallographically independent molecules in the asymmetric unit. Both molecules have the same co-ordination

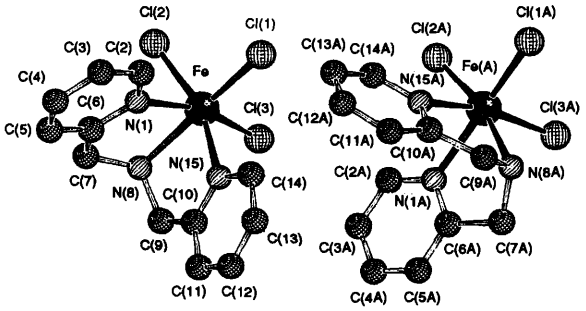

Fig. 1 Crystal structure of $[FeL^7Cl_3]$

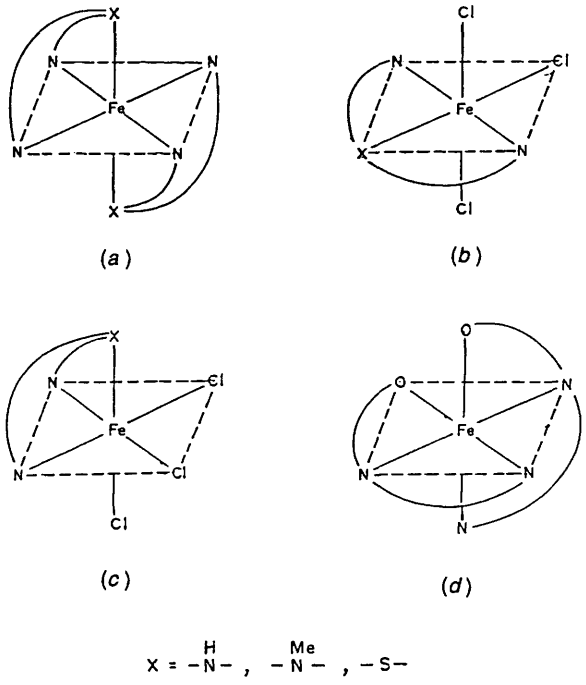

Fig. 2 Proposed structures of $[FeL_2]^{3+}$ (*a*) and $[FeLCl_3]$ complexes (*b*) and (*c*), where L = L^7–L^{11} and structure of $[FeL^{13}]^+$ (*d*)

geometry but the bond lengths and angles are slightly different. Each molecule is best described as a distorted octahedron in which the equatorial plane is defined by two *cis*-co-ordinated pyridine (py) nitrogens and two chloride ions. The secondary amine nitrogen is axial to this plane and *trans* to the third chloride ion resulting in folding and hence facial co-ordination of L^7 to Fe^{III}. Similar facial co-ordination of L^7 to low-spin Fe^{II} in $FeL^7{}_2(ClO_4)_2$[21] and to Cu^{II} in $CuL^7{}_2(BF_4)_2$[22] and that of L^8, the benzimidazole (bzim) analogue of L^7, to Cu^{II} in $CuL^8{}_2(ClO_4)_2 \cdot 2H_2O$[23] has been observed previously. The facial co-ordination of L^7 is in contrast to the meridional co-ordination of its *N*-methylamine bzim analogue L^9 observed in FeL^9Cl_3[17] and expected[23] in $[CuL^9{}_2]^{2+}$; it appears that the steric demand of the NMe group in L^9 changes[24] the orientation of its lone-pair orbital towards the metal ions and favours meridional co-ordination.

The two Fe–N_{py} bond lengths in one molecule are equal [2.168(14) and 2.172(13) Å] and similar to those in the other [2.197(14) and 2.194(13) Å] in the asymmetric unit. The heterocyclic rather than the secondary amine nitrogen as in the present compound [Fe–N_{amine} 2.216(13), 2.208(12) Å] or tertiary amine nitrogen as in FeL^9Cl_3[17] [Fe–N_{bzim} 2.082(8), 2.104(7), Fe–N_{amine} 2.374(7) Å] appears to be more strongly bound to high-spin Fe^{III} and as expected the secondary rather than the tertiary amine nitrogen is strongly bound in these compounds. This is in contrast to the situation in $[FeL^{12}{}_3]^{2+}$ [L^{12} = (2-aminomethyl)pyridine], where the amine rather than py nitrogen is strongly bound to high-spin iron(II) [Fe–N_{py} 2.223(5), Fe–N_{amine} 2.181(5) Å]. This presumably reflects the weaker σ interaction of the sterically hindered secondary compared to the primary amine nitrogen. Further, the Fe–N_{het} and Fe–N_{amine} bond distances in the present complex and in FeL^9Cl_3[17] are longer than those[22] [Fe–N_{py} 1.957(5), 1.978(4); Fe–N_{amine} 2.057(6) Å] in $FeL^7{}_2(ClO_4)_2$ with low-spin iron(II). This is expected because of the difference in the spin state of iron in these complexes.

As also found in FeL^9Cl_3, the three Fe–Cl bond distances in each molecule of the present structure are different, suggesting that the co-ordination geometry is rhombically distorted; this explains the low-field rhombic splitting of the $g = 4.3$ EPR signal (see below). The Fe–Cl(1) and Fe–Cl(2A) bonds which are *trans* to the amine nitrogen are the shortest of all the Fe–Cl bonds and this is expected for the weaker co-ordination of the secondary amine nitrogen. The two five-membered chelate rings pinch together the three bonds of the corresponding octahedral face so that the N–Fe–N bond angles are about 10–14° less than the 90° ideal, which is greater than those[22] (4–8°) for $[FeL^7{}_2]^{2+}$. Further, the angles at which the two py rings are canted are very close to complementary [73.6(4), 109.3(4)°]. This renders the two crystallographically independent molecules in the asymmetric unit apparently similar.

Structures of iron(III) complexes

All the iron(III) complexes have magnetic moments in the range 5.9–6.0 μ_B at room temperature, characteristic of a high-spin iron(III) centre. As in the crystal structures of $[FeL^7Cl_3]$ and FeL^9Cl_3,[17] the 1:1 complexes of L^{10} and L^{11} may be also octahedral with all the three chloride ions co-ordinated. The co-ordinated chloride ions are replaced by solvent molecules in solution, as revealed by conductometric studies. In all the 1:2 complexes, however, the chloride ion(s) are present in the outer sphere and hence the iron(III) can achieve six-co-ordination by binding to two tridentate ligand molecules.

The complexes $FeL^{13}{}_2ClO_4$[25] and $FeL^{13}{}_2PF_6$[26] {HL^{13} = *N*-[2-(imidazol-4-yl)ethyl]salicylaldimine} have been shown by crystal structure determination to possess octahedral structures with meridional co-ordination of the ligand [Fig. 2(*d*)]. Since the present phenolate ligands are analogous to L^{13}, it is reasonable to expect their bis complexes also to possess a similar octahedral structure. As in $[FeL^7{}_2(ClO_4)_2]$[21] the N_3 and N_2S ligands would be also expected to co-ordinate facially to iron(III) to generate octahedral structures [Fig. 2(*a*)]. In fact, L^8 and the N_2S ligand bis(imidazol-2-yl) thioether co-ordinate facially[23] to Cu^{II} to generate an octahedral structure. The corresponding 1:1 $FeLCl_3$ complexes would also involve facial co-ordination of L^8 and meridional or facial co-ordination of L^{10} and L^{11} [Fig. 2(*b*) and (*c*)]. Obviously, crystal structures of these complexes are essential to establish such predictions but it is unfortunate that suitable single crystals of them could not be grown.

Electronic absorption spectra

The main feature of the electronic spectra of the present bis chelates of tridentate phenolate ligands is the relatively intense band in the 450–630 nm region (Table 4, Fig. 3). This feature can be assigned to a charge-transfer transition from the p_π orbital on the phenolate oxygen to the partially filled d_π orbitals on iron.[27] This band is supplemented by a shoulder at higher energy (≈400 nm), which is also probably due to a charge-transfer transition.[27] The bands in the 300–350 nm region for the phenolate and other complexes are likely due to ligand π–π* transitions.

The lowest-energy phenolate-to-iron(III) charge-transfer (c.t.) band[27] is sensitive to the nature of the co-ordinating atoms, with the magnitude of the band energy in the order: $FeL^6{}_2$ > $FeL^2{}_2$ > $FeL^5{}_2$ > $FeL^3{}_2$ > $FeL^4{}_2$ > $FeL^1{}_2$. The band shifts to higher energies as the py nitrogen is replaced by the more

Table 4 Electronic spectral data[a] for iron(III) complexes in methanol solution

Compound	λ_{max}/nm (ε/dm^3 mol^{-1} cm^{-1})
$[FeL^1{}_2]Cl$	600 (sh) (530), 340 (sh) (7130)
$[FeL^2{}_2]Cl$	485 (1700), 400 (sh) (2190), 360 (5820)
$[FeL^3{}_2]Cl$	520 (720), 380 (2990), 320 (6640)
$[FeL^4{}_2]Cl$	580 (sh) (200), 330 (2210)
$[FeL^5{}_2]Cl$	495 (1840), 400 (2410), 350 (12 730)
$[FeL^6{}_2]Cl$	480 (990), 470 (1280), 400 (5190), 360 (8260)
$[FeL^7Cl_3]$	400 (sh) (430), 352 (830)
$[FeL^7{}_2Cl_3]$	370 (3490), 355 (sh) (2800)
$FeL^8Cl_3{\cdot}H_2O$[b]	436 (sh) (540), 358 (2780)
$FeL^8{}_2Cl_3$	360 (2690), 280 (16 690)
FeL^9Cl_3	357 (1490), 278 (9270)
$FeL^9{}_2Cl_3$	355 (2660), 280 (7350), 275 (12 550), 245 (15 150), 210 (18 230)
$[FeL^{10}Cl_3]$	330 (1489), 270 (3822)
$[FeL^{10}{}_2Cl_3]$	360 (2710), 280 (14 170), 270 (14 900), 240 (13 880), 210 (28 220)
$[FeL^{11}Cl_3]$	367 (1940), 335 (sh) (1560)
$[FeL^{11}{}_2Cl_3]$	360 (3190), 280 (17 160), 270 (16 830), 240 (12 080), 210 (26 790)

[a] Concentration of iron complexes $\approx 3.0 \times 10^{-3}$ mol dm^{-3}. [b] From ref. 9.

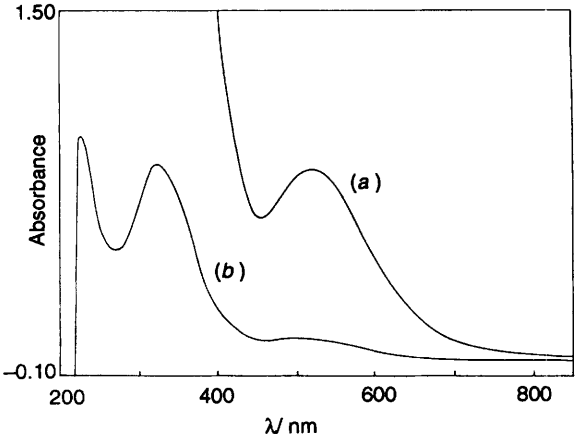

Fig. 3 Electronic absorption spectrum of $[FeL^3{}_2]Cl$ at 1.11×10^{-3} (*a*) and 1.23×10^{-4} mol dm^{-3} (*b*)

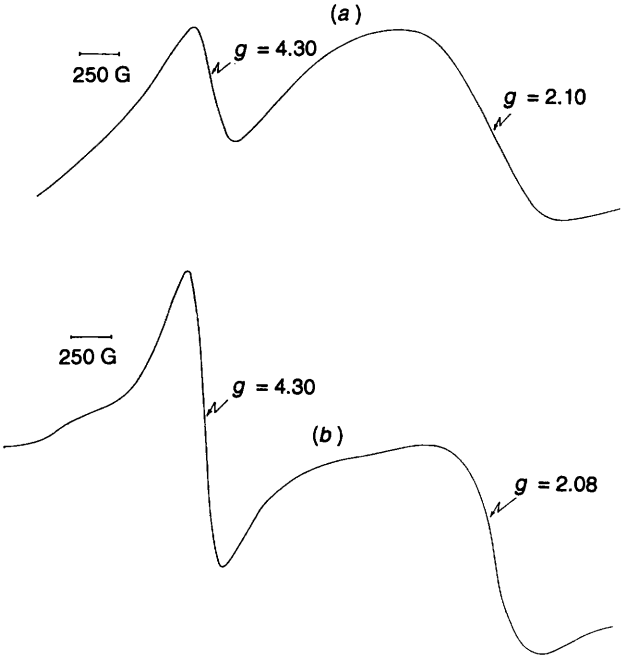

Fig. 4 X-Band EPR spectra of $[FeL^3{}_2]Cl$ (*a*) and $[FeL^6{}_2]Cl$ (*b*)

σ-donating bzim nitrogen and the six-membered chelate ring is replaced by a five-membered one which effects a stronger co-ordination. On the introduction of the NO_2 group as in $FeL^3{}_2$, the band energy decreases as expected;[9] however, for $FeL^5{}_2$ this is not observed, probably on account of the presence of the six-membered chelate ring which is expected to increase the band energy. Thus the decrease in Lewis acidity of the iron(III) centre is due to the increase in basicity of the donor atom which is expected[28] to raise the metal d-orbital energies, and hence the gap between the filled phenolate and the metal t_{2g} orbitals. Further, the c.t. band energy for a 1:2 chelate with two iron–phenolate bonds is expected to be higher than that for the corresponding 1:1 chelate. Thus $[FeL^1{}_2]Cl$ possesses a c.t. band of energy higher than that of FeL^1Cl_3.[9] The trend in the ligand-to-metal charge-transfer (l.m.c.t.) band energy is similar to that observed before,[9] but with exceptions.

EPR Spectra

The overall geometry of all the present complexes is octahedral and the donor atom set varies so widely that they are good systems to study the EPR spectral properties. The X-band EPR spectra of powder samples of all the phenolate and triaza ligand complexes (Figs. 4 and 5) exhibit broad (100–1900 G) signals near $g = 4.3$ and 2.0 at room temperature (Table 5), with relative intensities varying from complex to complex. The $g = 2$ signal may arise from spin–spin-coupled dimeric iron(III) species[29] the ground state of which, though diamagnetic at room temperature, may exhibit a transition at high temperatures. However, as in the crystal structure of $[FeL^7Cl_3]$, there is no evidence for Fe–Fe contact in the solid state. In this regard it is interesting that for the N_2S complexes this signal is much broader than those for other iron(III) complexes and the $g = 4.3$ resonance is not discernible. This may be due to broadening of the bands caused by increase in the relaxation time.[28]

The well resolved signal near $g = 4.3$ is typical of that predicted for a transition between the middle Kramer's doublet of rhombically distorted, high-spin monomeric iron(III) complexes. It is the most dominant spectral feature for the phenolate complexes and is characteristic of near-perfect rhombicity. For some of the complexes a splitting in the $g = 4.3$ signal is observed, as for the iron(III) tyrosinate proteins such as transferrins,[30] and for simple octahedral iron(III) complexes.[31] Thus the $g = 4.3$ signal is sensitive to the nature of the donor atoms determining the iron environment.

Electrochemical properties

All the complexes undergo $Fe^{III} \longrightarrow Fe^{II}$ reduction, as revealed by the magnitude of the current functions for the cathodic peaks (0.118 to −1.25 V, Tables 6 and 7, Figs. 6 and 7). Interestingly,

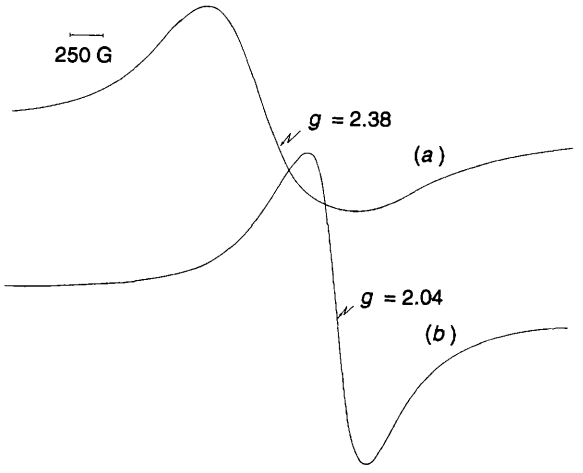

Fig. 5 X-Band EPR spectra of $[FeL^{10}Cl_3]$ (*a*) and $[FeL^{10}{}_2]Cl_3$ (*b*)

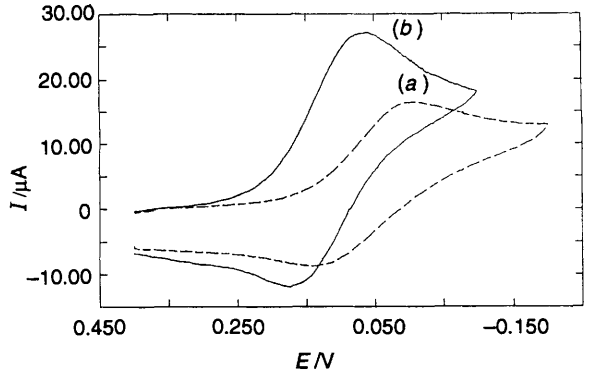

Fig. 6 Cyclic voltammograms of $[FeL^7Cl_3]$ (*a*) and $[FeL^7{}_2]Cl_3$ (*b*) in methanol. Supporting electrolyte: 0.1 mol dm^{-3} NBu_4ClO_4. Scan rate: 0.05 V s^{-1}

the bis(phenolate) complexes do not display the $Fe^{II} \longrightarrow Fe^{III}$ oxidation wave, suggesting that the iron(II) species generated are very unstable and that the redox cycle is completely irreversible. The ΔE_p values for the non-phenolate ligand complexes are much higher than the Nernstian value of 60 mV for a $n = 1$ process, suggesting that their redox chemistry tends to be non-Nernstian but is more reversible than that of the phenolates.

The following important features emerge from an analysis of Fe^{III}–Fe^{II} redox potentials. (*i*) The bis(phenolates) are reduced at potentials much more negative than those of the bis chelates of N_3 and N_2S ligands, obviously due to the co-ordination of more Lewis-base phenolates, which lowers the Lewis acidity of the iron(III) centre.[9] (*ii*) The redox potentials of the bis chelates of HL^1 and HL^5 are more negative than those of the corresponding 1 : 1 chelates, obviously due to the involvement of two phenolate donors in co-ordination. (*iii*) The $E_{\frac{1}{2}}$ of the bis(phenolates) vary in the order $FeL^3{}_2 > FeL^4{}_2 > FeL^5{}_2 > FeL^1{}_2 > FeL^2{}_2 > FeL^6{}_2$. Obviously, this reflects that bzim rather than py nitrogen is more strongly σ bonding. The five- rather than six-membered chelate ring is suitable to stabilize Fe^{III} and hence lowers the redox potential; however, the potentials of $FeL^3{}_2$ and $FeL^5{}_2$ are reversed, like their c.t. band energies. Thus the above order represents the change in Lewis acidity of the iron(III) centre, as modified by the ligand donor atoms. However, this order is not in agreement with that obtained on the basis of the phenolate-to-iron(III) c.t. band energies and such discrepancies are expected.[9] A plot of $\tilde{\nu}_{max}$ *vs.* $E_{\frac{1}{2}}$ does not give a linear correlation. It is reasonable to expect that some of the donor atoms in the six-co-ordinated complexes are replaced by chloride ions or solvent molecules in solution,

Table 5 Electron paramagnetic resonance spectral data for polycrystalline iron(III) complexes

Compound	g_2	ΔH_{pp}	g_1	ΔH_{pp}
$[FeL^1{}_2]Cl$	4.30	200	2.08	1250
$[FeL^2{}_2]Cl$	4.30	200	2.14	640
$[FeL^3{}_2]Cl$	4.30	238	2.10	925
$[FeL^4{}_2]Cl$	4.30	150	2.00	500
$[FeL^5{}_2]Cl$	4.27	288	—	—
$[FeL^6{}_2]Cl$	4.30	200	2.08	650
$[FeL^7Cl_3]$	—	—	2.16	1750
$[FeL^7{}_2Cl_3]$	4.30	75	2.19	1875
$[FeL^8Cl_3]^a$	4.22	325	2.01	350
$FeL^8{}_2Cl_3$	4.31	125	2.06	750
$[FeL^9Cl_3]^b$	—	—	2.05	525
$FeL^9{}_2Cl_3$	4.30	140	2.00	1600
$[FeL^{10}Cl_3]$	—	—	2.38	1150
$[FeL^{10}{}_2Cl_3]$	—	—	2.04	500
$[FeL^{11}Cl_3]$	—	—	2.00	250
$[FeL^{11}{}_2Cl_3]$	—	—	2.03	950

[a] Data consistent with ref. 9. [b] From ref. 17.

Table 6 Electrochemical data[a] for iron(III) bis complexes of phenolate ligands in acetonitrile at 25 ± 0.2 °C, scan rate 50 mV s^{-1}

Compound	E_{pc}	$E_{\frac{1}{2}}{}^b$	$E_{\frac{1}{2}}{}^c$	$i_{pc}{}^d$/μA
$[FeL^1{}_2Cl]$	−0.944	−0.726	−0.893	18.3
$[FeL^2{}_2Cl]$	−0.356	—	−0.295	18.0
			−0.946	
$[FeL^3{}_2Cl]$	−0.560	−0.401	−0.476	13.2
$[FeL^4{}_2Cl]$	−0.786	−0.639	−0.654	9.0
$[FeL^5{}_2Cl]$	−1.080	−0.764	−0.740	21.8
$[FeL^6{}_2Cl]$	−1.250	−0.980	−1.105	53.6

[a] *E*/V *vs.* Ag–$AgNO_3$ (0.01 mol dm^{-3}, 0.1 mol dm^{-3} NBu_4ClO_4); add 0.544 V to convert to *E vs.* NHE. [b] Potential at half height. [c] Pulse height 50 mV (differential pulse voltammetry). [d] Cyclic voltammetry.

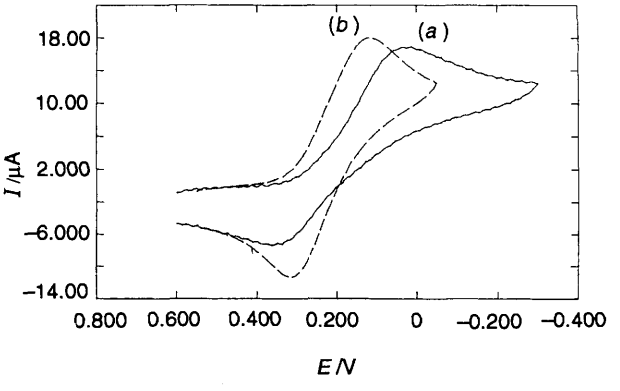

Fig. 7 Cyclic voltammograms of $[FeL^{11}Cl_3]$ (*a*) and $[FeL^{11}{}_2]Cl_3$ (*b*) in methanol. Conditions as in Fig. 6

affecting the Lewis acidity. (*iv*) Both the 1 : 1 and 1 : 2 complexes of L^{10} exhibit $E_{\frac{1}{2}}$ values which are not greatly different from those of the corresponding triaza ligand (L^8) complexes. This suggests that the tendency of the weakly co-ordinating thioether donors to stabilise Fe^{III} over Fe^{II} is not different from that of the secondary amine nitrogen. This observation is similar to that made for analogous 1 : 2 copper(II) complexes.[23] (*v*) The bis chelates, except $[FeL^7{}_2]Cl_3$, are generally harder[23] to reduce (140–300 mV) than are the corresponding 1 : 1 complexes, obviously due to the increased stabilisation of Fe^{III} by the greater number of ligand donor atoms. Thus the redox potential of $FeL^9{}_2Cl_3$ is much more negative than that of $[FeL^9Cl_3]$.

Table 7 Electrochemical data* for the iron(III) mono and bis complexes of aza and thioether ligands in acetonitrile at 25 ± 0.2 °C, scan rate 50 mV s^{-1}

Compound	E_{pc}	E_{pa}	ΔE_p	$E_{\frac{1}{2}}$ CV	$E_{\frac{1}{2}}$ DPV[b]	$i_{pc}/\mu A$
$[FeL^7Cl_3]$[c]	−0.007	0.140	151	0.068	0.054	13.0
$[FeL^7{}_2Cl_3]$[c]	0.062	0.174	112	0.118	0.127	27.1
$[FeL^8Cl_3]$	0.062	0.140	68	0.101	0.101	16.7
$FeL^8{}_2Cl_3$	−0.310	−0.110	200	−0.210	−0.196	7.0
$[FeL^9Cl_3]$	0.072	0.220	148	0.146	0.148	11.9
$FeL^9{}_2Cl_3$	−0.824	−0.648	176	−0.736	−0.727	43.4
$[FeL^{10}Cl_3]$	0.012	0.116	104	0.065	0.070	9.8
	−0.202					12.8
$[FeL^{10}{}_2Cl_3]$	−0.314	0.116	198	−0.215	−0.190	3.9
	−0.652					
$[FeL^{11}Cl_3]$	0.118	0.312	194	0.215	0.222	18.0
$[FeL^{11}{}_2Cl_3]$	0.022	0.356	334	0.189	0.135	16.8

[a] E/V *vs.* Ag–$AgNO_3$ (0.01 mol dm^{-3}, 0.1 mol dm^{-3} NBu_4ClO_4); add 0.544 V to convert to E *vs.* NHE. [b] Differential pulse voltammetry, pulse height 50 mV. [c] Measured in methanol solution.

Conclusion

The present study leads to the conclusion that in 1 : 1 complexes bis(pyridin-2-ylmethyl)amine is folded facially to co-ordinate to iron(III) while, in contrast, the corresponding bis(benzimidazol-2-ylmethyl)methylamine binds meridionally. The analogous bis(benzimidazol-2-yl)-aza and -thioether ligands have been suggested to co-ordinate facially to iron(III) in 1 : 1 and 1 : 2 complexes. All the present complexes display quite interesting spectral behaviour and Fe^{III}–Fe^{II} redox chemistry. The Lewis acidity of the iron(III) centre in these complexes, as derived from the phenolate-to-iron(III) c.t. band energies and Fe^{III}–Fe^{II} redox potentials, is dictated by the donor functionalities. The present high-spin bis(phenolate) complexes with FeN_4O_2 chromophores exhibit rhombic $g = 4.3$ signals. They have been suggested to possess a rhombically distorted octahedral structure around high-spin iron(III). This is interesting because the naturally occurring tyrosinate proteins such as transferrins and lactoferrins also exhibit rhombic $g = 4.3$ signals and the crystal structure of human lactoferrin[32–35] shows a rhombically distorted octahedral environment around iron.

Acknowledgements

We thank the Council of Scientific and Industrial Research, New Delhi, for financial support [Grant No. 9(299)90 EMR II] and for a fellowship to one of us (R. V.) [9/475(25)91 EMR I] and the Regional Sophisticated Instrumentation Centre, Indian Institute of Technology, Madras for EPR and X-ray diffraction facilities. Dr. B. Varghese and Mr. T. Manisekaran are thanked for X-ray data collection. The University Grants Commission, New Delhi, is thanked for granting a Teacher Fellowship (to T. B.) and for the Career Award (to P. T. M.).

References

1 D. D. Cox and L. Que, jun., *J. Am. Chem. Soc.*, 1988, **110**, 8085.
2 Y. Nishida, H. Shimo and S. Kida, *J. Chem. Soc., Chem. Commun.*, 1984, 1611.
3 L. Que, jun., and R. H. Heistand, II, *J. Am. Chem. Soc.*, 1979, **101**, 2219.
4 R. H. Heistand, II, R. B. Lauffer, E. Fikrig and L. Que, jun., *J. Am. Chem. Soc.*, 1982, **104**, 2789.
5 L. Que, jun., *Coord. Chem. Rev.*, 1983, **50**, 73.
6 D. H. Ohlendorf, J. D. Lipscomb and P. C. Weber, *Nature (London)*, 1988, **336**, 403.
7 A. E. True, A. M. Orville, L. L. Pearce, J. D. Lipscomb and L. Que, jun., *J. Am. Chem. Soc.*, 1990, **29**, 10 847.
8 R. Viswanathan, M. Palaniandavar, T. Balasubramanian and T. P. Muthiah, to be published.
9 R. Viswanathan and M. Palaniandavar, *J. Chem. Soc., Dalton Trans.*, 1995, 1259.
10 J. W. Pyrz, A. L. Roe, L. J. Stern and L. Que, jun., *J. Am. Chem. Soc.*, 1985, **107**, 614.
11 A. B. P. Lever, *Inorg. Chem.*, 1990, **29**, 1271 and refs. therein.
12 T. M. Aminabhavi, N. S. Biradar and S. B. Patil, *Inorg. Chim. Acta*, 1986, **125**, 125.
13 E. C. Horning, *Organic Synthesis*, Wiley, New York, 1955, vol. 3, p. 468.
14 M. A. Philips, *J. Chem. Soc.*, 1928, 2393; S. Usha, T. Pandiyan and M. Palaniandavar, *Indian J. Chem., Sect. B*, 1993, **32**, 572.
15 A. W. Addison and P. J. Burke, *J. Heterocycl. Chem.*, 1981, **18**, 803.
16 J. V. Dagdigian, V. McKee and C. A. Reed, *Inorg. Chem.*, 1982, **21**, 1332.
17 H. Adams, N. A. Bailey, J. D. Crane, D. E. Fenton, J.-M. Latour and J. M. Williams, *J. Chem. Soc., Dalton Trans.*, 1990, 1727.
18 G. M. Sheldrick, SHELXS 86, Program for Automatic Structure Solution, Göttingen, 1986.
19 G. M. Sheldrick, SHELXL 93, University of Göttingen, 1993.
20 M. Nordelli, *Comput. Chem.*, 1983, **7**, 95.
21 R. J. Butcher and A. W. Addison, *Inorg. Chim. Acta*, 1989, **158**, 211.
22 M. Palaniandavar, A. W. Addison and R. J. Butcher, *Inorg. Chem.*, 1996, **34**, 467.
23 M. Palaniandavar, T. Pandiyan, M. Lakshminarayanan and H. Manohar, *J. Chem. Soc., Dalton Trans.*, 1995, 455 and refs. therein.
24 Y. Nishida and K. Takahashi, *J. Chem. Soc., Dalton Trans.*, 1988, 691.
25 L. Que, jun., R. H. Heistand, II, R. Mayer and A. L. Roe, *Biochemistry*, 1980, **19**, 2588.
26 J. C. Davis, W.-J. Kung and B. A. Averill, *Inorg. Chem.*, 1986, **25**, 394.
27 M. D. Timkin, D. N. Hendrickson and E. Sinn, *Inorg. Chem.*, 1985, **24**, 3947.
28 A. W. Addison and C. G. Wahlgren, *Inorg. Chim. Acta*, 1988, **147**, 61.
29 L. Borer, L. Thalken, C. Ceccarelli, M. Glick, J. Zhang, II, and W. M. Reiff, *Inorg. Chem.*, 1983, **22**, 1719; L. Borer, L. Thalken, J. Zhang, II and W. M. Reiff, *Inorg. Chem.*, 1983, **22**, 3174.
30 E. W. Ainscough, A. M. Brodie, J. E. Plowman, S. J. Bloor, J. Sanders-Loehr and T. M. Loehr, *Biochemistry*, 1980, **19**, 4072.
31 W. T. Oosterhuis, *Struct. Bonding (Berlin)*, 1974, **20**, 59; M. I. Scullane, L. K. White and N. O. Chasteen, *J. Magn. Reson.*, 1982, **47**, 383; R. Aasa, *J. Chem. Phys.*, 1970, **52**, 3919; E. J. Nanni, jun., M. D. Stallings and D. T. Sawyer, *J. Am. Chem. Soc.*, 1980, **102**, 4481.
32 B. F. Anderson, H. M. Baker, E. J. Dodson, G. E. Norris, S. V. Rumball, J. M. Waters and E. N. Baker, *Proc. Natl. Acad. Sci. USA*, 1987, **84**, 1769.
33 B. F. Anderson, H. M. Baker, M. Haridas, G. E. Norris, S. V. Rumball, C. A. Smith and E. N. Baker, *Abstracts, XXVIIth International Conference on Coordination Chemistry*, Brisbane, 1989, S20.
34 S. Bailey, R. W. Evans, R. C. Garratt, B. Gorinsky, S. Hasnain, C. Horsburgh, H. Jhoti, P. F. Lindley, A. Mydin, R. Sarra and J. L. Watson, *Biochemistry*, 1988, **27**, 5804.
35 P. K. Bali and W. R. Harris, *J. Am. Chem. Soc.*, 1989, **111**, 4457.

Received 3rd *January* 1996; *Paper* 6/00052E